# Underwater Robot Localization Using Magnetic Induction: Noise Modeling and Hardware Validation

Javier Garcia*, Steban Soto*, Arifa Sultana, Julien Leclerc, Miao Pan, and Aaron T. Becker

***Abstract*— Localization is a fundamental task in many swarm robotic applications, such as foraging and exploration. Magnetic induction communications, which rely on the magnetic component of an antenna's near-field, have gathered interest as means to perform localization in underground and underwater environments. MI signals propagate through lossy environments better than traditional RF signals, and can offer advantages over acoustics. In prior work, we developed a localization method based on MI signals to calculate the range between two moving MI antennas. A core aspect of the method is a particle filter that relies on the received signal strength and speed of the antennas to produce location estimates. In this paper, we first empirically find the amount of noise present in our signal strength measurements in underwater environments. Then we propose a model to capture the impact of the noise on the range calculations and apply it to improve the particle filter's location estimations.**

## I. Introduction

Subsea localization for autonomous underwater vehicles (AUV) serves as a gateway enabling many other applications, including offshore rig inspection and environmental monitoring. These applications are possible through the deployment of underwater wireless sensor networks (UWSN) with multi-agent robot systems for data collection or inspection. These systems have potential advantages in affordability, scalability, and the lack of single points-of-failure.

Multiple solutions to localization in above-ground environments exist, relying on methods such as computer vision and traditional RF communications. However, these methods face challenges for underground and underwater environments, where visibility can be non-existent and RF signals attenuate quickly due to the lossy characteristics of the media. Magnetic induction (MI) signals have recently been used to overcome such difficulties in short range applications, where they are less susceptible to attenuation. The hardware required to implement MI communications is also simpler and cheaper compared to acoustics, a popular technology underwater.

Our hardware implementation relies on the use of triaxial coil antennas to estimate the relative location of a robot based on measured voltage data. These antennas are typically used for MI communications and have been tested in air and underwater. In previous work we showed the feasibility of reconstructing the path a robot takes around another in air using triaxial antennas and a particle filter. However, noise present in the environment was represented by values with no experimental basis. In this work, we study how the inclusion of a noise model based on empirically obtained values improves localization accuracy.

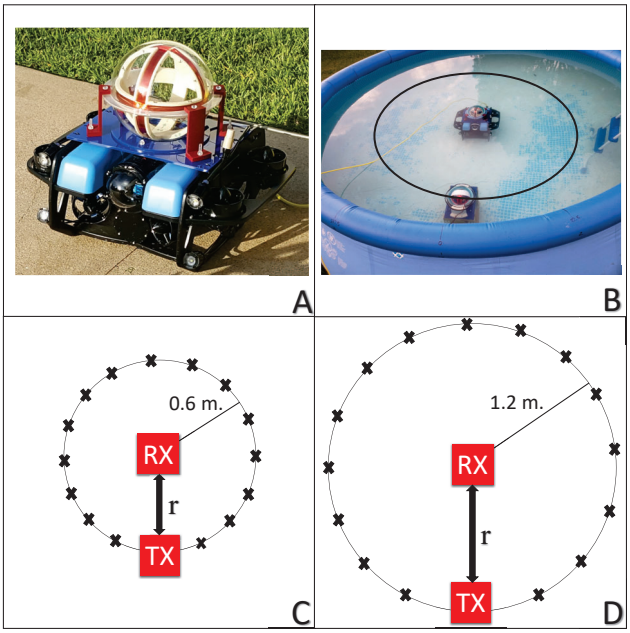


Fig. 1. Small scale pool setup. A: A BlueROV2 equipped with a triaxial coil antenna. B: Small-scale experiment setup. C: Circular path with a radius of 0.6 [m]. D: Circular path with a radius of 1.2 [m]. Measurements were taken in increments of 22.5 degrees. The range between the antennas is represented by $r$.

This work is arranged as follows: In Section II we present several avenues of research related to this work. The theory and experiment setup are shown in Section III, and the results from our experiments are shown in Section IV. We conclude the work in Section V.

## II. Related Work

Using magnetic induction for communications have been studied over the years as an alternative for underwater systems. Recent surveys can be found from [1] and [2].

Due to the UWSN applications for MI communications, localization methods often require multiple nodes to increase accuracy. This is true not only for MI-based methods but also for acoustic methods. For example, long-baseline (LBL) systems, short-baseline (SBL), and ultra-short-baseline (USBL) positioning systems rely on multiple transponders for positioning and bearing calculations [3]. Despite its low data rate, high transmission delay, and expensive deployment costs,

* These authors contributed equally to the paper.

* This project was paid for in part with federal funding from the Department of the Treasury through the State of Texas under the Resources and Ecosystems Sustainability, Tourist Opportunities, and Revived Economies of the Gulf Coast States Act of 2012 (RESTORE Act) and the National Science Foundation under Grant No. [1646607]. The content, statements, findings, opinions, conclusions, and recommendations are those of the author(s) and do not necessarily reflect the views of the State of Texas or the Treasury.

Global Oceans 2020: Singapore - U.S. Gulf Coast | 978-1-7281-5446-6/20/$31.00 ©2020 IEEE | DOI: 10.1109/IEEECONF38699.2020.9389237

its high range makes acoustic communications the preferred approach for underwater communications and localization.

Current research for localization using acoustic communications include Kalman filters [4], particle filters [5], [6], and hybrids between acoustic and RF-based methods [7]. The authors of [5] performed bearing-only localization between AUVs that have magnetometer and acceleration sensors installed on the receiver AUV for pose measurements. Their particle filter then uses these measurements to estimate the location of the robot that carries the receiver based on direction information provided by the transmitting robot. This approach eliminates the requirement for a real-time clock for synchronization. However, since the transmitter is required to stay at a fixed position, large errors occur due to drift and initial conditions.

Alternatively, Erol et al. proposed an AUV-assisted approach that relies on the robot to gather GPS information while on the surface before diving and following a predetermined trajectory in order to locate all nodes [8]. The robot and sensor nodes share a common communication protocol to transmit location information so that the nodes can localize themselves using triangulation or the bounding box method, with pressure sensors installed for depth calculations. This approach allows sensor nodes to be deployed arbitrarily. Synchronization between them is not required.

The use of coil antennas solely for localization have been studied for over fifty years, most notably starting with Kalmus' work on magnetic guidance and tracking [9] and Raab's work using triaxial antennas [10].

For localization with MI communications, two or more nodes are used to improve accuracy. These nodes, often named *anchor nodes*, are stationary and their position is known with respect to the environment. Adding more anchor nodes improves accuracy, getting as low as 10 [cm] accuracy with eight anchor nodes [11].

Our work is related to Huang and Zheng's paper, which studies the localization of a single triaxial coil with respect to two transmitting coils whose position is known [12]. The three coils of each transmitting antenna are excited sequentially, resulting in sixteen possible solutions for the location of the coil, which are then reduced by generating rotation matrices, then applying maximum likelihood estimation. Alternatively, the authors present a distance-based method, where the minimum mean square error metric is applied to estimate the location of the coil. While this method does not completely solve the multiple solutions problem, it is computationally less complex.

This paper only considers the use of one anchor node to represent the localization between two robots. This reduces the accuracy of our estimates and increases the chance of location ambiguity. By using a particle filter, we can produce a reasonable estimate of the robot's state over time using the data from the triaxial antenna. Furthermore, the performance of the particle filter improves by considering data from an onboard sensor, such as using data from an inertial measurement unit (IMU).

## III. Methods

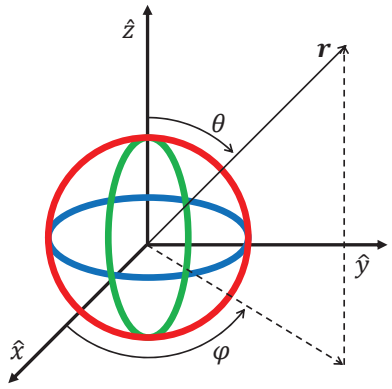


Fig. 2. Representation of our MI triaxial antennas.

This paper analyzes the ambient noise in an underwater medium to extend the work in [13]. Our antennas are composed of three orthogonal wire coils, as shown in Fig.2. We utilize the same amplifier circuitry for the transmissions.For the receiver, we use a National Instruments (NI) CompactRIO controller with the NI-9220 voltage input module to measure the differential voltages induced on the receiving coils.

### A. Fundamental Theory

We paraphrase the theory used in the work from [13] below. We assume that the magnetic fields are quasistatic and model our coils as magnetic dipoles.

The magnetic field strength by coil $i$ at a point designated by $\mathbf{r}$ is

$$h_i(\mathbf{r}) = \frac{1}{4\pi|\mathbf{r}|^3}[3\hat{r}(\mathbf{m}\cdot\hat{r}) - \mathbf{m}], \tag{1}$$

where $\mathbf{m}$ is the magnetic moment of the dipole. For a coil antenna, the magnetic moment is $\mathbf{m} = NIA\hat{u}$, where $N$ is the number of wire turns, $I$ is the current flowing through the wire, $A$ is the area of the coil and $\hat{u}$ is the unit vector perpendicular to that area.

Since $\mathbf{m} = |\mathbf{m}|\hat{m}$, (1) is rewritten as

$$h_i(\mathbf{r}) = \frac{|\mathbf{m}|}{4\pi|\mathbf{r}|^3}[3\hat{r}(\hat{m}\cdot\hat{r}) - \hat{m}], \tag{2}$$

We split the magnetic field strength into its components such that $h_i(\mathbf{r}) = \begin{bmatrix} h_{i,x} & h_{i,y} & h_{i,z}\end{bmatrix}$. Similarly, $\hat{r} = \begin{bmatrix} r_x & r_y & r_z\end{bmatrix}$ and $\hat{m} = \begin{bmatrix} m_{i,x} & m_{i,y} & m_{i,z}\end{bmatrix}$. If we define $q_i = \widehat{m_i}\cdot\hat{r}$, then the $x$ component of the magnetic field strength due to coil $i$ is given by

$$\begin{aligned} h_{i,x} &= \frac{|\mathbf{m}|}{4\pi|\mathbf{r}|^3}[3r_x(\hat{m}_i\cdot\hat{r}) - m_{i,x}] \\ &= \frac{|\mathbf{m}|}{4\pi|\mathbf{r}|^3}[3r_x q_i - m_{i,x}]. \end{aligned} \tag{3}$$

To extract the magnitude of $\mathbf{r}$, which is the main quantity required by the particle filter, we begin by finding the norm

of the magnetic field produced by the transmitting coil $i$. The norm of $h_i$ is given by

$$\begin{aligned}|h_i| &= \sqrt{(h_{i,x})^2 + (h_{i,y})^2 + (h_{i,z})^2} \\ &= \frac{|\mathbf{m}|}{4\pi|\mathbf{r}|^3}\sqrt{(3r_x q_i - m_{i,x})^2 + (3r_y q_i - m_{i,y})^2 + (3r_z q_i - m_{i,z})^2} \\ &= \frac{|\mathbf{m}|}{4\pi|\mathbf{r}|^3}\sqrt{3(q_i)^2 + 1}. \end{aligned} \tag{4}$$

Since the three transmitting coils are orthogonal, the vector $\mathbf{q} = \begin{bmatrix} q_1 & q_2 & q_3 \end{bmatrix}$ is also a unit vector. By assuming that the magnitude of the magnetic moment of all three coils is the same we get the following system of linear equations:

$$\begin{aligned} 3\left(\frac{|h_1|}{|h_2|}\right)^2 (q_2)^2 + \left(\frac{|h_1|}{|h_2|}\right)^2 &= (3q_1)^2 + 1 \\ 3\left(\frac{|h_1|}{|h_3|}\right)^2 (q_3)^2 + \left(\frac{|h_1|}{|h_3|}\right)^2 &= (3q_1)^2 + 1 \\ (q_1)^2 + (q_2)^2 + (q_3)^2 &= 1 \end{aligned} \tag{5}$$

By solving for $\mathbf{q}$ the magnitude of $\mathbf{r}$ can be calculated from (4), if the values for the magnetic field components are known. This results in

$$|\mathbf{r}| = \left(\frac{C}{|h_x|^2 + |h_y|^2 + |h_z|^2}\right)^{\frac{1}{6}}, \tag{6}$$

where $C$ is the constant related to the magnetic moment magnitude $|\mathbf{m}|$.

### B. Noise Measurements

We performed tests in three different environments to obtain the voltage measurements to be analyzed. The first environment was a small and shallow pool. The receiving antenna was placed in the center of the pool while the transmitting antenna was moved around it in two circular paths of different radii. The setup is shown in Fig. 1. The second environment was a portion of NASA's Neutral Buoyancy Lab (NBL), where the antennas were placed at a depth of about 5 [m]. The last environment was an open area in Lake Conroe, located northwest of the city of Houston, with the receiving antenna located at varying depths. Measurements from the receiving antenna were continuously recorded for the last two environments, with no predetermined paths followed.

To calculate the noise, we considered the cases where we expect no received signal, such as when the transmitter is off or a particular receiving coil is orthogonal to the currently transmitting coil. The voltages measured in such cases correspond in part to the noise present in the environment. Other effects such as the inaccuracy of our magnetic field model and measurement errors contribute to the non-zero measured voltages, but are neglected in this work. The average noise values for each receiving coil for all environments were computed.

### C. Noise Model

Equation (6) only considers the magnetic field values $h_i$ directly calculated from the voltages measured at the receiving coils $i = 1, 2, 3$. In order to incorporate the noise data, we first modify the magnetic field expressions using the linear hypothesis [14]

$$h_{i,r} = h_{i,t} + \sigma^2_{h,i} = \frac{v_{i,t} + \sigma^2_{v,i}}{\mu_0 \omega N A}, \tag{7}$$

where $v_{i,t}$ is the noiseless component of the voltage received, $\sigma^2_{v,i}$ is the noise component, $\omega$ is the frequency of the system, and $N$ and $A$ are the number of wire turns and face area of the coils. With the noise taken into account, (6) is now

$$|\mathbf{r}| + \sigma^2_{|\mathbf{r}|} = \left(\frac{C}{h^2_{x,r} + h^2_{y,r} + h^2_{z,r}}\right)^{\frac{1}{6}} = C^{\frac{1}{6}}(H + \Sigma)^{-\frac{1}{6}}, \tag{8}$$

where $H = h^2_{x,t} + h^2_{y,t} + h^2_{z,t}$ and $\Sigma = 2(h_{x,t}\sigma_{h,x} + h_{y,t}\sigma_{h,y} + h_{z,t}\sigma_{h,z}) + \sigma^2_{h,x} + \sigma^2_{h,y} + \sigma^2_{h,z}$. We are interested in extracting the terms containing noise values, since they are the only terms contributing to $\sigma^2_\rho$. Using the binomial theorem for negative exponents [15], we obtain the following approximation ($|\Sigma| < H$)

$$\sigma^2_{|\mathbf{r}|} = C^{\frac{1}{6}}\left(-\frac{1}{6}\Sigma H^{-\frac{7}{6}} + \frac{7}{72}\Sigma^2 H^{-\frac{13}{6}}\right). \tag{9}$$

This derivation shows that the uncertainty present in our range calculation method depends both on the ambient noise and on the magnetic fields at the receiver. The particle filter calculates the ideal magnetic fields for the particles being considered, so there is no issue with $H$ being part of the expression for $\sigma^2_{|\mathbf{r}|}$.

## IV. Results

The noise values calculated from the test data sets are shown in Table I below. The data sets from the two different circular paths in the shallow pool are considered as two different environments. The values cover a range of a few millivolts, with the noisiest cases less than 7 [mV].

TABLE I

$\sigma^2_{v,i}$ VALUES

| | X coil [mV] | Y coil [mV] | Z coil [mV] |
|---|---|---|---|
| **Pool-0.6 [m] circle** | 5.21 | 6.04 | 6.92 |
| **Pool-1.2 [m] circle** | 4.03 | 4.54 | 5.27 |
| **Lake Conroe** | 4.71 | 3.19 | 4.79 |
| **NBL** | 1.99 | 1.64 | 1.14 |

To test the effects of the noise model on localization performance, we incorporate it into our existing particle filter. The algorithm reads the data sets from the circular paths in the shallow pool and estimates the location of the transmitting antenna as it moves. Additionally, we use data sets previously obtained in tests performed in a larger pool. These data sets correspond to a 3 [m] square path and a 3 [m] boustrophedon path, whose setup is shown in Fig.4.

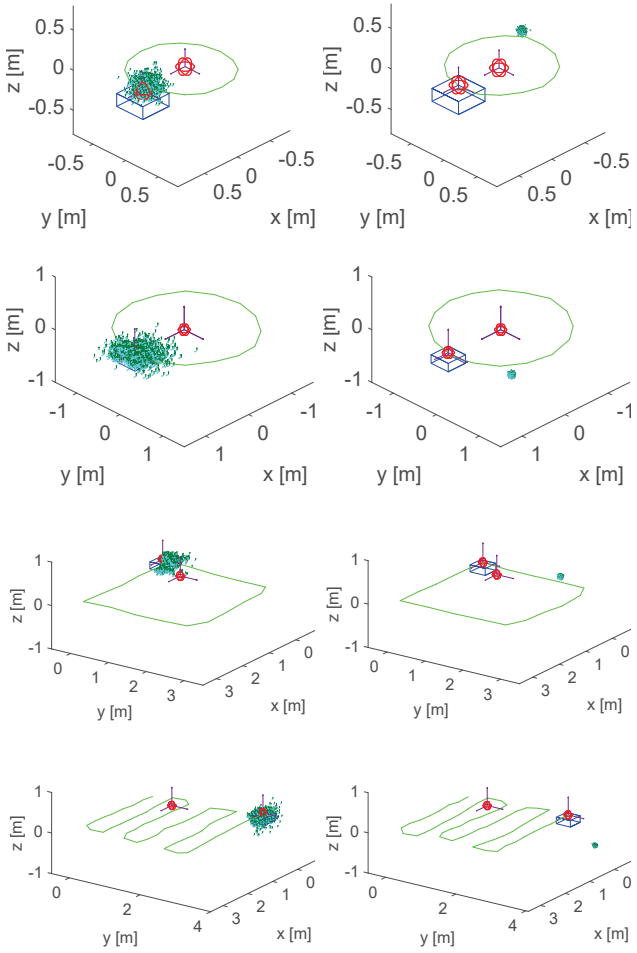


Fig. 3. Representative final estimations of the particle filter for multiple paths. From top-down: Circle path with radius 0.6 [m], circle path with radius 1.2 [m], square path with side length 3 [m], and the boustrophedon path. With noise (left), the particle cloud is spread out and contains some good estimates of the antenna. Without noise (right) the particle cloud is more compact but far away from the true antenna position.

Fig. 3 shows the final estimates produced by the filter for the 0.6 [m] circular path, the 1.2 [m] circular path, the 3[m] square path and the 3 [m] boustrophedon path, considering noise and assuming no noise present. The estimates are represented by the green/blue cloud of particles. In all cases, the noise values used are those in the second row of Table I. Without noise the resulting particle cloud is considerably compact at the end of the path, but is not accurate in estimating the final position of the transmitting antenna. In contrast, with the noise taken into account the resulting particle cloud is more spread out at the end, but contains reasonable estimates for both paths. Although the noise values were computed from data obtained in a different environment, they work well with the 3 [m] square and 3 [m] boustrophedon path, indicating that the noise does not vary enough to impede the performance of the filter.

The effect of the noise value is further demonstrated in Fig. 5, where the errors between the true state of the transmitting antenna and the filter's most likely particle

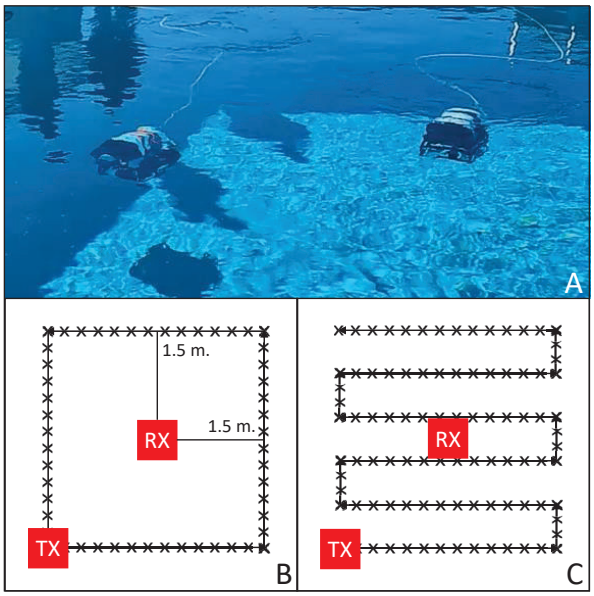


Fig. 4. Larger pool experiment setup. A: Coils mounted inside waterproof buckets, carried by two BlueROV2 robots. B: Square path with side length of 3 [m]. C: Boustrophedon path with side length of 1 [m] and 0.6 [m] step length.

(MLP) for different scenarios are plotted. Besides the cases of no noise and noise equal to the calculated $\sigma^2_{v,i}$, two more cases are considered where the calculated $\sigma^2_{v,i}$ was amplified and attenuated by a factor of 10. In all cases, the filter was run 10 times, and the mean and standard error for each of the 16 measurement locations (iterations) was computed.

The MLPs resulting from using the calculated $\sigma^2_{v,i}$ have a smaller error by the end of the paths on average. The filter performs similarly well with the attenuated values, having only a slightly worse error. For the amplified values, the error is considerably worse, and its standard deviation is larger. Not considering noise at all results in an error comparable to the size of the circular path, and doesn't change much through the course of the iterations.

## V. Conclusion

In this work we derived a model for incorporating the voltage noise received by a triaxial coil antenna, in different underwater environments, into an equation used to calculate the range between two such antennas based on measured induced voltages. The model parameters for two circular paths of different radii were obtained by considering certain data points measured at different locations along said paths, according to the simplified quasi-static approximation used in our MI-based approach. We also performed measurements in larger bodies of water, ultimately showing that the geometry of the environment did not heavily impact the calculated noise values

A particle filter recreated the circular paths considering different values for the noise, as well as other paths performed in a larger pool. The error between the best estimate and the true state of the antenna was smallest for the values

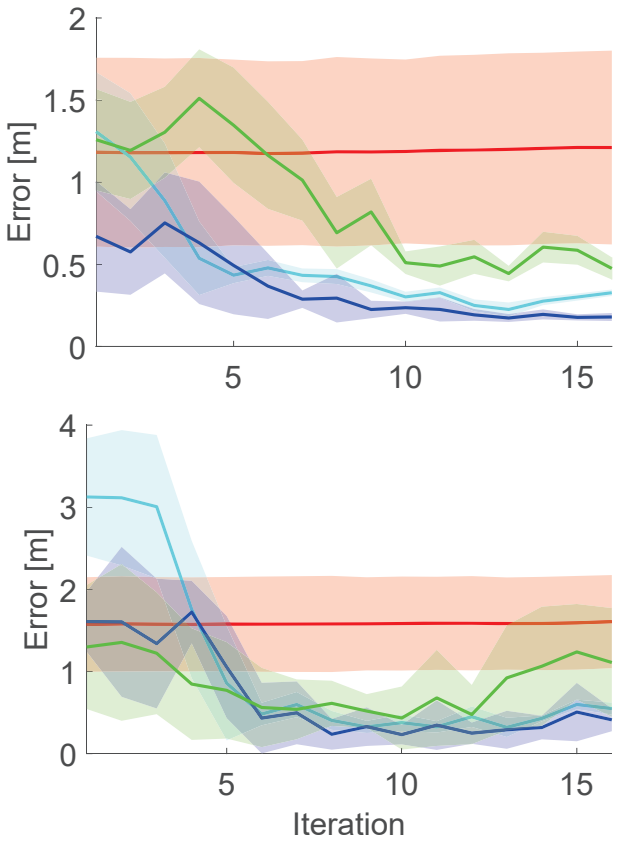


Fig. 5. Average error between the filter's MLP and the true state of the robot for the 0.6 [m] path (top) and the 1.2 [m] path (bottom). The colors correspond to no noise (red), $0.1\sigma^2_{v,i}$ (cyan), $\sigma^2_{v,i}$ (blue) and $10\sigma^2_{v,i}$ (green).

calculated from the derived noise model, followed closely by the same values attenuated by a factor of 10. As the noise values were amplified, the error became much worse. However, not considering noise at all resulted in worst error for all paths, indicating a useless estimation. The trend observed is that noise values equal to and smaller than, within a certain range, the ones resulting from the model are beneficial in producing good estimates.

## References


[1] Y. Li, S. Wang, C. Jin, Y. Zhang, and T. Jiang, "A Survey of Underwater Magnetic Induction Communications: Fundamental Issues, Recent Advances, and Challenges," *IEEE Communications Surveys Tutorials*, February 2019.

[2] M. Muzzammil, N. Ahmed, G. Qiao, I. Ullah, and L. Wan, "Fundamentals and advancements of magnetic field communication for underwater wireless sensor networks," *IEEE Transactions on Antennas and Propagation*, pp. 1–1, 2020.

[3] L. Zhou, "A precise underwater acoustic positioning method based on phase measurement," Master's thesis, University of Victoria, 2010.

[4] J. Kim, "Cooperative localization and unknown currents estimation using multiple autonomous underwater vehicles," *IEEE Robotics and Automation Letters*, vol. 5, no. 2, pp. 2365–2371, 2020.

[5] K. Fujita, T. Matsuda, and T. Maki, "Bearing only localization for multiple auv with acoustic broadcast communication," in *2019 19th International Conference on Control, Automation and Systems (ICCAS)*, Oct 2019.

[6] Y. Xu, W. Dandan, and F. Hua, "Underwater acoustic source localization method based on tdoa with particle filtering," in *The 26th Chinese Control and Decision Conference (2014 CCDC)*, 2014, pp. 4634–4637.

[7] J. Espinosa, M. Tsiakkas, D. Wu, S. Watson, J. Carrasco, P. R. Green, and B. Lennox, "A hybrid underwater acoustic and rf localisation system for enclosed environments using sensor fusion," in *Towards Autonomous Robotic Systems*, M. Giuliani, T. Assaf, and M. E. Giannaccini, Eds. Springer International Publishing, 2018.

[8] M. Erol, L. F. M. Vieira, and M. Gerla, "Auv-aided localization for underwater sensor networks," in *International Conference on Wireless Algorithms, Systems and Applications (WASA 2007)*, Aug 2007.

[9] H. P. Kalmus, "A new guiding and tracking system," *IRE Transactions on Aerospace and Navigational Electronics*, vol. ANE-9, no. 1, pp. 7–10, 1962.

[10] F. H. Raab, E. B. Blood, T. O. Steiner, and H. R. Jones, "Magnetic position and orientation tracking system," *IEEE Transactions on Aerospace and Electronic Systems*, vol. AES-15, no. 5, pp. 709–718, Sep. 1979.

[11] G. Dumphart, H. Schulten, B. Bhatia, C. Sulser, and A. Wittneben, "Practical accuracy limits of radiation-aware magneto-inductive 3d localization," in *2019 IEEE International Conference on Communications Workshops (ICC Workshops)*, May 2019, pp. 1–6.

[12] H. Huang and Y. R. Zheng, "Node localization with aoa assistance in multi-hop underwater sensor networks," *Ad Hoc Networks*, vol. 78, pp. 32 – 41, 2018. [Online]. Available: http://www.sciencedirect.com/science/article/pii/S1570870518302178

[13] J. Garcia, S. Soto, A. Sultana, and A. Becker, "Localization using a Particle Filter and Magnetic Induction Transmissions: Theory and Experiments in Air," in *2020 IEEE Texas Symposium on Wireless & Microwave Circuits & Systems*, May 2020.

[14] A. L. Edwards, *An Introduction to Linear Regression and Correlation*. San Francisco, CA: W. H. Freeman, 1976.

[15] E. W. Weisstein, "Negative binomial series," https://mathworld.wolfram.com/NegativeBinomialSeries.html.